Resources, Conservation & Recycling 172 (2021) 105666

Contents lists available at ScienceDirect

Resources, Conservation & Recycling

journal homepage: www.elsevier.com/locate/resconrec

Full length article

Innovative recycling of organic binders from electric vehicle lithium-ion batteries by supercritical carbon dioxide extraction

Yuanpeng Fu [a,b], Jonas Schuster [a,c], Martina Petranikova [a], Burçak Ebin [a,*]

[a] Chalmers University of Technology, Department of Chemistry and Chemical Engineering, Nuclear Chemistry and Industrial Material Recycling, S-412 96 Gothenburg, Sweden
[b] China University of Mining and Technology, School of Chemical Engineering & Technology, Xuzhou 221116, Jiangsu, China
[c] Hamburg University of Technology

ARTICLE INFO

Keywords:
Lithium-ion batteries
Cathode material
Supercritical CO_2
Dimethyl sulfoxide
Liberation

ABSTRACT

The growing demand for energy storage devices due to the skyrocketing production/consumption of portable electrical and electronic equipment as well as electric vehicles has promoted battery technologies, resulting in the piling of a large number of waste lithium-ion batteries (LIBs). Organic binders wrapped on electrode particles are usually the main reason that causes the difficulty of liberation and extraction of electrode materials. Pyrolysis or incineration is the general approach to separate the organic binder, leading to fluorinated exhaust gas emissions. In this study, the supercritical carbon dioxide (SC CO_2) combined with a cosolvent dimethyl sulfoxide was innovatively adapted to enable the extraction of organic binders from spent LIBs to facilitate the liberation of the cathode material from aluminum foil. Pure polyvinylidene fluoride was preferentially used to study the SC CO_2 dissolution mechanism. The results indicate that 98.5 wt% polyvinylidene fluoride (PVDF) dissolves in SC CO_2 dimethyl sulfoxide system under the optimum conditions; 70°C process temperature, 80 bar pressure, and 13 min duration. After removing PVDF, the recovered sample was characterized by Fourier Transform Infrared Spectrometer (FTIR) and thermogravimetric analyzer (TGA) to observe its possible re-utilization. It is clear that the surficial chemical groups and content remained the same after treatment. SC CO_2 processing effectively liberates the active cathode material from the aluminum substrate due to removal of the binder. The suggested innovative approach is promising as an alternative pretreatment method due to its high efficiency, relatively low energy consumption, and environmentally friendly features.

1. Introduction

The gradual popularity of consumer electronics and electric vehicles initiate a transaction in portable energy storage devices that LIBs gradually became a kind of major power source due to the preferable electrochemical characteristic and relatively long service-life (Shin et al., 2005, Ramanayaka et al., 2020). It is worth noting that electrical vehicles have bright prospects and are widely used in the automotive manufacturing industry, which leads to large amount of lithium-ion battery cathode materials (i.e., $LiNi_{1/3}Mn_{1/3}Co_{1/3}O_2$, $LiNi_{0.5}Mn_{0.3}Co_{0.2}O_2$, etc) (Fu et al., 2019, Kasnatscheew et al., 2018). The global annual manufacturing of LIBs was around 13.8 GWh in 2014 and increased to 173.5 GWh in 2020 (Projected lithium ion battery market size worldwide in 2017 and 2025 2019). There are different approximations for their service life when batteries are in use, considering the first application and the second-life for another purpose instead of going to waste stream. In electric vehicle (EV) applications, the LIBs are usually deemed discarded when their discharge capacity was lower than 70% of the initial capacity (Zhang et al., 2015). After the end-of-life of LIBs, the inappropriate disposal of spent batteries can pose a serious threat to the environment due to their hazardous components, such as transition metals, electrolytes, and other organic components (Meng et al., 2018, Shi et al., 2018). On the other hand, battery waste is a valuable secondary source because the grades of valuable metals (Li, Co, Ni, Mn, etc.) in them are much higher than natural raw ores (Meshram et al., 2015, Meshram et al., 2015, Fu et al., 2019). Therefore, creative green recycling approaches to recover the major components of the spent LIB serves not only to minimize waste and possible hazardous materials but also to activate resource utilization and support sustainable production.

* Corresponding author.
E-mail addresses: fuyuanpeng@cumt.edu.cn (Y. Fu), jonas.schuster@online.de (J. Schuster), burcak@chalmers.se (B. Ebin).

https://doi.org/10.1016/j.resconrec.2021.105666
Received 18 November 2020; Received in revised form 2 May 2021; Accepted 6 May 2021
Available online 24 May 2021

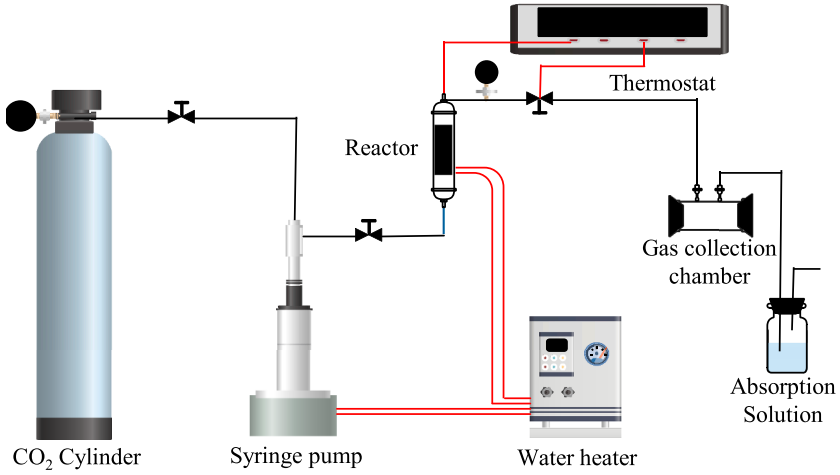

Fig. 1. Scheme of the SC CO_2 system for the recovery of spent LIBs

It is widely accepted that a pretreatment process to separate organic binders from spent LIBs and liberate the electrode active materials is necessary for subsequent hydrometallurgical recycling processes. It usually includes discharging, dismantling, and separation of the components, and the electrode active materials (Yang et al., 2015). Separation of electrode active materials from copper and aluminum current collectors is a critical stage to ease the material recovery (Zhang et al., 2018). Existing technologies to achieve the liberation between the electrode material and aluminum/copper foils are mechanical crushing (Ku et al., 2016, Zhang et al., 2013), ultrasonic cleaning (Li et al., 2009), organic solvent dissolution (Xin et al., 2016, Nayaka et al., 2016), and high temperature processes (Hao et al., 2014, Choi and Kim, 2012). These methods were technically sufficient to remove the PVDF binder and liberate the electrode active materials from the substrate. However, in terms of economic and environmental factors, the high energy consumption and handling with toxic chemicals and exhaust geases are the bottleneck of the the processes . Chemical removal and high temperature treatment approaches have crucial drawbacks considering environmental concerns and workplace safety. The generation of hydrofluoric acid (HF) and fluorine rich organic compounds, as well as lower molecule chain fluorinated organics such as vinylidene fluoride and 1,1,1,3,3,3-hexafluoro-propane, etc. (Lombardo et al., 2020, Zhang et al., 2018, Hanisch et al., 2015) must be additionally treated to elliminate the pollution and minimized the environment impact of high temperature processing. In case of solvent dissolution and ultrasonic cleaning approaches, the most widely used chemicals such as NMP are toxic and highly dangerous for workers and the environment (Risk Evaluation for N-Methylpyrrolidone (NMP) 2016), and ultrasonic cleaning is not suitable for industrialized manufacture due to its low treatment capacity. Additionally, the mentioned methods fail to consider organic binder recovery or obtains reusable PVDF. The above problems limit the use of these processes in spent LIBs recycling.

As a new hydrometallurgical technology, supercritical fluid was recently implemented to recycle valuable components from WEEE (Lv et al., 2018, Grützke et al., 2015, Sanyal et al., 2013, Xiu and Zhang, 2009, Xing and Zhang, 2013), and the successful results encourage investigations on battery recycling. SC fluid is an unusual solvent since the organic solubility is manipulated by pressure and temperature, which leads to extraction above the critical point and releasing below it (Wang et al., 2017, Cooper, 2000). The characteristics of the SC fluid, such as low viscosity, high mass transport coefficient, high diffusivity, and high solubility of organics, are the key benefits to implement this technique for the dissolution of organic and metals (Lin et al., 2014, Xiang et al., 2014). These characteristics of SC fluid make it easier to extract organics and metals from spent LIBs compared with other hydrometallurgical methods. Carbon dioxide, as a common solvent for supercritical fluid, is recently studied for metal recovery because of its several advantages comparing to other solvents such as water, ethanol, acetone, etc. (Herrero et al., 2010, Erkey, 2000). SC CO_2 is a good low-cost solvent without any secondary pollution and non-flammable. Additionally, CO_2 has a relatively low supercritical point, 31 °C and 74 bar (Xiu and Zhang, 2009, Baek et al., 2016). The dissolution of organic materials in SC CO_2 is more favorable than the other SC fluids, especially in a proper cosolvent system due to relatively high diffusivity (Lin et al., 2014, Liu et al., 2017). Thus, research on the recycling of transition metals and organic chemicals from waste LIBs by supercritical carbon dioxide (SC CO_2) technology has become increasingly attractive due to its uniqueness to minimize the hazardous effects of the recovery process to the environment (Lv et al., 2018).

Several processes utilize SC fluids for the metal's recovery of the valuable components from spent LIBs and separate its components by removing the polymers (Nowak and Winter, 2017, Argenta et al., 2017). As reported by Grützke (Grützke et al., 2015, Grützke et al., 2014), a yield of 89.1 wt% electrolyte (composition of DMC, EMC and EC) was achieved by extraction for 30 min with SC CO_2 (25 °C, 60 bar) and 0.5 mL/min acetonitrile/propylene carbonate. Bertuol (Bertuol et al., 2016) applied SC CO_2 for the leaching of cobalt contained in lithium-ion batteries (LIBs). In their study, leaching tests were performed with SC CO_2 and cosolvents in comparison with conventional conditions. The use of supercritical conditions enables the extraction of more than 95 wt.% of the cobalt, with minimized reaction time, and required concentration of H_2O_2 compared to the conventional leaching at atmospheric pressure. Although some studies focused on the implementation of SC fluid technology for different parts of the battery recycling, there is still a lack of systematic investigation to understand the value of the technology in the recycling field to eliminate the hazardous process waste and minimize the environmental side effects. Besides, there have been no previous studies concerning the application of supercritical fluids in the removal of PVDF from spent LIBs.

In this study, SC CO_2 fluid technology was adapted to dissolve and separate the organic binder of LIB cathodes in a cosolvent due to the desirable characteristics of the technology considering economic and environmental factors. The research aims to achieve an efficient liberation of the cathode materials from aluminum foil by removing organic binders. Meanwhile, PVDF material was recovered without destroying properties and reusable characteristics. The dissolution of pure PVDF under SC CO_2 fluid was investigated to reveal the mechanism, including chemical composition, surficial properties, and dissolution effect. Then, actual cathode material was used to propose a recycling process for spent LIBs with lower chemical consumption and needed operation

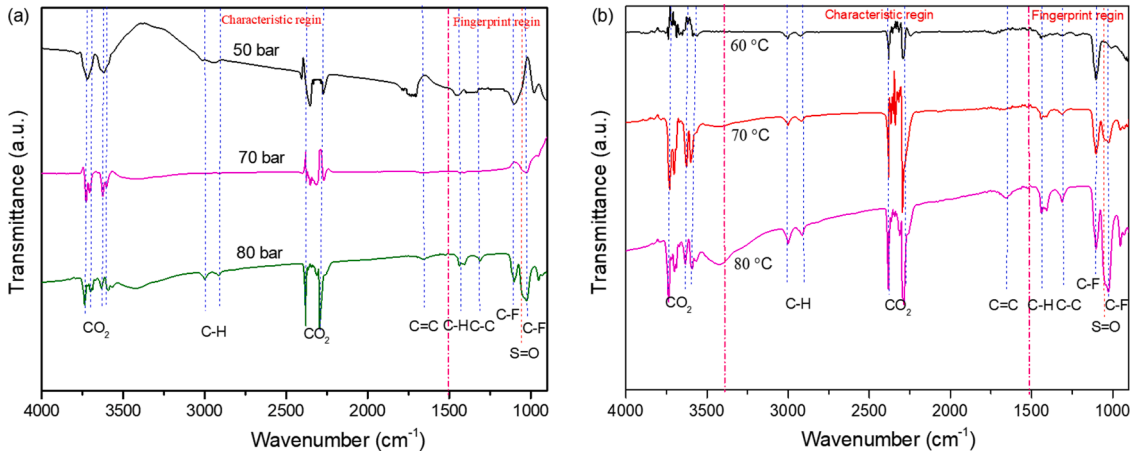

Fig. 2. FT-IR spectra of the exhaust gas samples under different (a) pressure at 80°C for 15 min, (b) temperature at 80 bar and 15 min

conditions and high recycling efficiency.

2. Experimental

2.1. Materials and reagents

Pure PVDF material was supplied by a synthetic materials corporation, and the plate material was cut into pieces and used for subsequent experiments. The reagent DMSO (analytically pure) was purchased from Sigma-Aldrich, Ltd, and its nontoxicity was identified from the Material Safety Data Sheet (MSDS). CO_2 (purity 99.998%) was used for extraction experiments. The spent aluminum laminated batteries (ALBs) used in this study were provided by a vehicle manufacturing company. Firstly, the batteries were discharged in 10% NaCl solution (w/v) 24 h to prevent possible accidents and fire during dismantling stage. Then they were manually dismantled into different components to obtain the anode and cathode foils. The obtained cathode foils were cut into 1×1 cm^2 pieces and used for the subsequent SC CO_2 extraction process. Cathode material was then treated by aqua regia (HCl: $HNO_3 = 3{:}1$) and filtered and diluted (3 times) for elemental analysis by inductively coupled plasma optical emission spectrometry (ICP-OES, iCAP 6000 series, Thermo Scientific). The results are given in Table S1. The composition of the test sample by XRD (Fig.S1) was found to be $LiNi_{1/3}Co_{1/3}Mn_{1/3}O_2$, $LiMn_2O_4$ and carbon.

2.2. Experimental procedures

The supercritical fluid experimental set-up used for the supercritical carbon dioxide (SC CO_2) dissolution of PVDF and spent LIBs extraction was constructed inside of the fume hood and illustrated in Fig. 1. An ISCO syringe pump and controller (Teledyne ISCO model 260D, Lincoln, NE, USA) was used in the experiments. A liquid CO_2 bottle was connected to the syringe pump to load the pump and then the desired pressure was set. Three valves were used to connect and control the CO_2 flow, and of which the outlet valve of the reactor was heated by a thermostat to avoid the frozen during pressure reliefs. The samples and cosolvents were located in a reactor constructed of 316 stainless steel and were fixed by an iron pedestal. The stainless steel reactor was heated via a thermostat water bath to keep the temperature of the reaction system stable. Besides, the temperature of CO_2 was controlled at the given temperature by heating the syringe pump column using a thermostat before introducing the reactor.

For each experiment, supercritical conditions were adjusted at a given temperature and pressure for CO_2. Firstly, about 0.5 g solid PVDF or cathode material were added into the reactor that contains a 4 mL cosolvent DMSO solution. Then the reactor was closed and tighten to avoid the gas leakage. The experiment will start timing once the temperature and pressure keep stable at set point. To obtain the optimum conditions, various pressure (40-90 bar), temperature (40-90°C), and duration time (4-17 min) were in turn tested during the SC CO_2 process. Then the exhaust gas sample was collected in a gas collection chamber for approximately 30 seconds during the pressure releasing. For the liquid sample, the samples in the reactor that contained dissolved PVDF were directly collected after the extraction vessel cooling to room temperature. The dissolved PVDF precipitated in cosolvent at room temperature and pressure. The dissolved and precipitated PVDF in cosolvent were extracted by centrifugal operation. The residual PVDF and cathode powder materials were collected from the reactor and characterized by followed electron microscopy and sieving analysis. All experiments were triplicated to obtain reliable data. The mean values of the results are used in the graphs and the standard deviations were added in the followed results curve. Additionally, PVDF dissolution in DMSO at 70°C for 13 min in the atmospheric environment was investigated to compare with SC CO_2 treatment.

2.3. Measurement and characterization

The surface morphology and elements of raw electrode materials and the SC CO_2 treatment products were studied by scanning electron microscope (SEM-EDS, Phenom Pro X, Phenom) under back scattered electrons mode. Process exhaust gas samples and organic component PVDF remains were characterized using a Perkin Elmer Spectrum Two FTIR spectrometer equipped with a deuterated triglycine sulfate (DTGS) detector and with a monolithic diamond ATR accessory (PerkinElmer, UATR two). Prior to sample measurement, the mixture of DMSO solvent with CO_2 was collected by an empty run and then measured under 50-60 bar pressure, and used as background gas for FTIR studies of exhaust gas samples. The thermogravimetric analyzer (TGA, Q500, TA) was used to determine and compare the thermochemical properties of the raw PVDF and SC-CO_2 recovered PVDF materials. The concentrations of different metals in solution were determined by inductively coupled plasma optical emission spectrometry. The dissolution and recovery efficiencies of

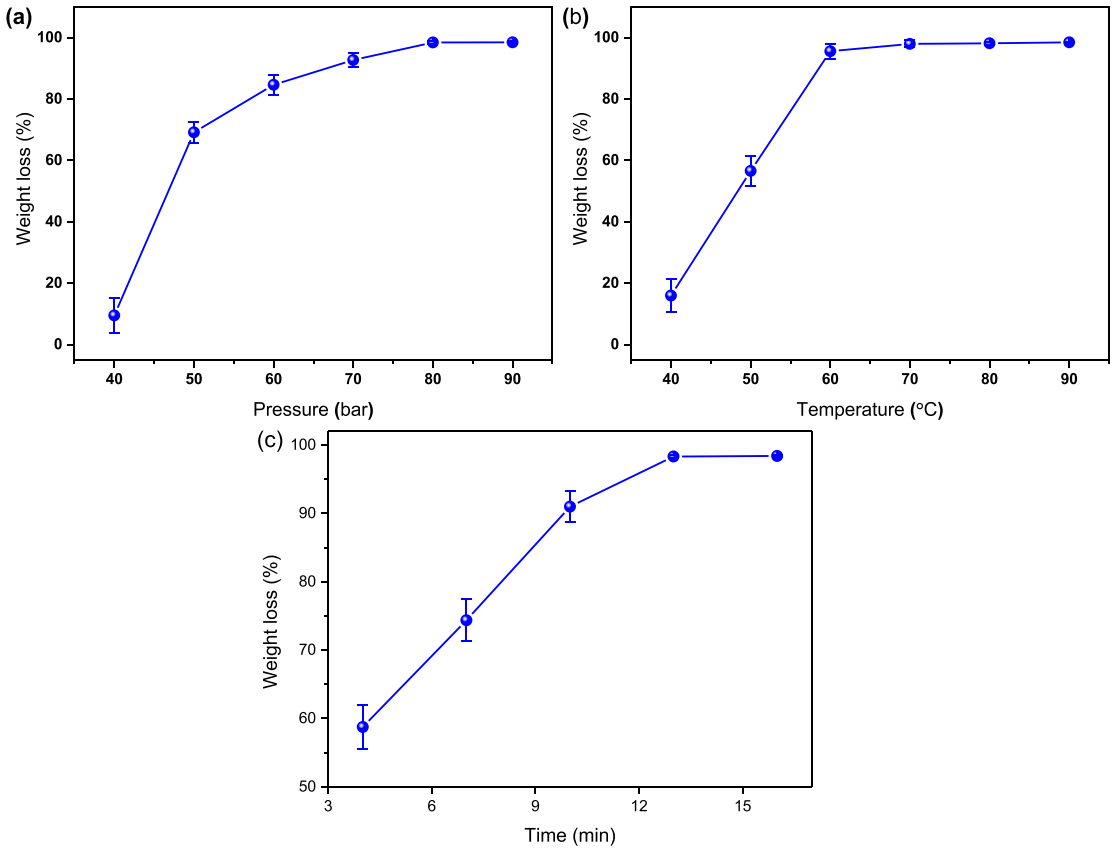

Fig. 3. Weight loss of raw PVDF as functions of (a) pressure under 80°C and 15min, (b) temperature under 80 bar and 15 min and (c) time under 70°C and 80 bar of SC CO_2 with DMSO as cosolvent

PVDF can be calculated according to Eqs. (1) and (2), respectively:

$$E = 1 - \frac{m_a}{m_0} \times 100\% \quad (1)$$

$$R = \frac{m_1}{m_0} \times 100\% \quad (2)$$

Where E is the dissolution efficiency (%), m_a is the weight of the remained PVDF after the dissolution process, and m_0 is the total weight of the PVDF before dissolution. R is the recovery efficiency (%) of PVDF extracted from the cooled solution, where m_1 is the weight of the recovered PVDF as (dissolved, separated, and then precipitated).

3. Results and discussion

3.1. Dissolution of pure PVDF under supercritical CO_2 fluid

To explore the feasibility of PVDF dissolution under supercritical carbon dioxide (SC CO_2)-DMSO system, the collected exhaust gas samples after extraction were analyzed by FTIR and the spectrums are given in Fig. 2. The region of the whole spectra is divided into characteristic (1500-4000 cm^{-1}) and fingerprint (400-1500 cm^{-1}) regions. It is observed that the spectra present the characteristic peaks for DMSO at 1057 cm^{-1}, which belongs to S=O bond. The two characteristic regions observed in 3750 cm^{-1}-3550 cm^{-1} and 2450 cm^{-1}-2250 cm^{-1} belong to C-O stretching vibration, which is attributed to the CO_2 in SC fluid (Marr and Gamse, 2000). In the fingerprint region, the peaks at 1103 cm^{-1} and 1022 cm^{-1} belong to the anti-symmetrical and symmetrical stretching vibration of the C-F bond, respectively (Nieuwoudt et al., 2014). Besides, it is clear that the peaks 2925 cm^{-1} and 2855 cm^{-1} are corresponding to anti-symmetrical and symmetrical stretching vibration of methylene C-H bond, and the peak at 1440 cm^{-1} belongs to methylene C-H bending vibration (He et al., 2015). They were usually used to identify the chemical bonds and functional groups of PVDF binder. As shown in Fig. 2a, the peaks of the C-H bond did not appear until the pressure increased to 80 bar. Meanwhile, the dissolution effect can be enhanced by adjusting operation temperature and pressure as presented by the increasing intensity of the characteristic peaks of PVDF. The peak at 1653 cm^{-1} belongs to the C=C stretching vibration of alkene, which means that partly degradation of PVDF polymers can possibly occur and generate alkene monomers. While this peak is not clear at lower temperatures until it becomes obvious at 80°C and 80 bar. Based on the above analysis, the FTIR results indicate that it is feasible to dissolve PVDF with DMSO solvent under SC CO_2 process. The experimental parameter range including temperature, pressure and time were further investigated to obtain the optimal PVDF dissolution effect below.

The effect of experimental conditions on pure PVDF dissolution was investigated under the pressure range 40-90 bar and 40-90°C process temperatures for different durations (4-17 min). The experimental point curve (error bars: Mean±SD) of the weight loss of PVDF is presented in Fig. 3 for the PVDF-CO_2-DMSO system. The effect of pressure on weight loss of PVDF is shown in Fig. 3a, the experiments were conducted for 15 min duration time at 80°C. The weight loss remarkably increased by pressurizing the reactor from 40 to 80 bar. There was a slight change in the sample dissolution when the pressure increased from 80 to 90 bar. Fig. 3b indicates the effect of temperature on PVDF dissolution under the conditions of 80 bar and 15 min. Although the dissolution of the sample was limited at 40°C, which is around 18.6% weight loss of PVDF, increasing the temperature accelerated the process leading to the almost complete dissolution of the sample in the SC CO_2 and DMSO cosolvent system. The results show an effective weight loss of PVDF when temperature and pressure exceed the critical point, which is attributed to the

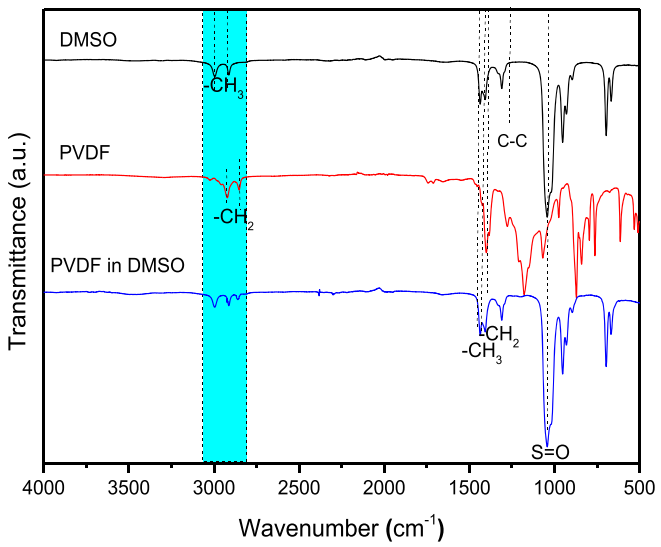

Fig. 4. FTIR spectra of DMSO and dissolved PVDF in DMSO by Sc-CO_2 at 80 bar and 70°C for 13 min

Table 1
Comparison for optimal dissolution and recovery effect of PVDF under 70°C and 13 min

Items	SC-CO_2 process	Room pressure process
Pressure /bar	80	Room pressure
Dissolution rate /%	98.5	8
Recovery rate /%	97.5	-

improved dissolution of PVDF by cosolvent DMSO. It is known that the density of SC CO_2 was increased under higher pressure (He et al., 2015), in which the interaction between PVDF and solvent was accordingly enhanced. Besides, a higher temperature (>60°C) does not help a lot to improve the diffusion coefficient of the solvent. Fig. 2c presents the effect of time on PVDF dissolution at 80 bar and 70°C process conditions. It can be seen that the optimal dissolution was reached for 13 min process duration, where the weight loss of PVDF reached 98.5%.

The above FTIR spectra reveal that part of the solid PVDF was transformed into gas during dissolution in DMSO and SC CO_2 system and carried out together with exhaust gas stream by releasing the pressure. Besides, it is also necessary to characterize the dissolved PVDF in liquid samples that were collected from the reactor. Firstly, pure DMSO and pure solid PVDF were characterized by FTIR and then the liquid sample, which is dissolved PVDF in DMSO by SC CO_2 at 80 bar and 70°C for 13 min, was measured, as given in Fig. 4. The peaks of the DMSO spectrum at 3010 cm^{-1} and 2915 cm^{-1} are attributed to the anti-symmetrical and symmetrical stretching vibration of methyl C-H bond, and the peak at 1440 cm^{-1} and 1405 cm^{-1} belongs to methyl C-H bending vibration respectively. Besides, the peak at 1057 cm^{-1} belongs to S=O bond. After SC CO_2 DMSO fluid process, it is obvious that the peaks of the C-H appeared in its spectrum due to the dissolution of PVDF in the DMSO solution. Considering the mass loss, and FTIR studies, it can be concluded that the optimal condition to dissolve PVDF by SC-CO_2 and DMSO system solution 70°C temperature, 80 bar pressure at 13 min using 125 g/L (S/L) ratio. While in comparison, the weight loss of PVDF is only 8% at 60°C and for 13 min in DMSO at room pressure (Table 1). The optimal experimental conditions of SC CO_2 fluid will be adapted for the subsequent liberation of actual cathode materials.

3.2. Recycling and characterization of dissolved PVDF

3.2.1. TG characterization of PVDF before and after SC CO_2 extraction

The solid PVDF was almost completely dissolved in the DMSO solution by SC CO_2 extraction. After releasing the pressurized CO_2 and cooling the liquid sample at room temperature, 99 wt% of the dissolved PVDF precipitated in the DMSO and recovered. From the starting material, 97.5 wt% of the PVDF was retrieved by the proposed SC CO_2 treatment. The recovery of PVDF without changed properties and high efficiency is of significance in the whole extraction process. Thermogravimetric analyses (TGA) were performed to determine the organic composition of the samples. Fig. 5 shows the TGA results of the raw PVDF and the recovered material after cooling the DMSO solution process. The weight loss and its derivative as a function of temperature are graphed in the TGA curves, and the characteristic thermal behavior was clearly observed at temperatures between 400 and 550°C. These two peaks are referred to as the thermal decomposition of PVDF (Zhan et al., 2020). The position and shape of the two characteristic peaks of the recovered PVDF did not change. Meanwhile, the weight loss of the recovered PVDF with increasing temperature is nearly the same as the raw material.

3.2.2. Morphology and functional groups analysis

The morphology and surface functional groups of the raw PVDF and recovered products after the precipitation in DMSO process were investigated by SEM and FTIR. The raw PVDF material presents a condensed morphology, as observed in Fig. 6. After the SC CO_2 extraction process, the recovered material has a loose morphology embraced by a large number of fibrous PVDF slivers. Meanwhile, it shows almost no difference in peak shape and position for FTIR spectra between raw and recovered PVDF, especially for the peaks lower than 100 cm^{-1}. Based on the above analysis, the recovered PVDF maintained similar properties includes chemical components and surficial functional groups. It means that only morphological changes took place, probably due to degradation to smaller molecular chains during the dissolution and extraction of PVDF during the SC CO_2 process. Besides, PVDF is generally accepted as partly crystalline, and chain disentanglement during the dissolution can be irreversible for the crystalline polymers after removing the solvent (Talebi, 2008), which can cause changes in the morphology. Considering the results, separation of PVDF material with similar chemical properties, unchanged properties and reusable characteristics is possible by the suggested recycling process. Thus, it is a promising process to remove and recover the organic binders from spent LIBs using supercritical fluid technology.

3.2.3. Mechanism of SC CO_2 on PVDF recovery

The reaction mechanism of PVDF dissolution in DMSO under SC CO_2 was proposed according to the experimental and characterization results as presented in Fig. 7. The solute-solvent interaction gradually occurs with three steps. For the first step, the PVDF plate was surface-adsorbed by DMSO and of which partly dissolved. Then PVDF plate was dissolved into pieces, in which the solvent was more easily able to pass through the PVDF matrix. Besides, as presented in the right side graph of Fig. 7, it presents a special property of a supercritical fluid that its density is close to liquid while viscosity similar to gas (Bachu, 2008). Additionally, Brownian movement of the whole liquid system also shows an enhancement attributed to the increase of temperature, which enhanced the proportion of collision of PVDF under the SC solvent. For the final step, the solid PVDF was dissolved and changed into long chain compound.

Compared with the alternative conventional gas-liquid interface, the interface of the supercritical CO_2 system disappears, and thus, the fluid is converted into non-condensable gas. In general, the dissolution behavior of PVDF was effectively improved by adjusting the pressure and temperature of the supercritical CO_2 -DMSO system. The superior characteristic of supercritical CO_2 such as high diffusivity, low viscosity,

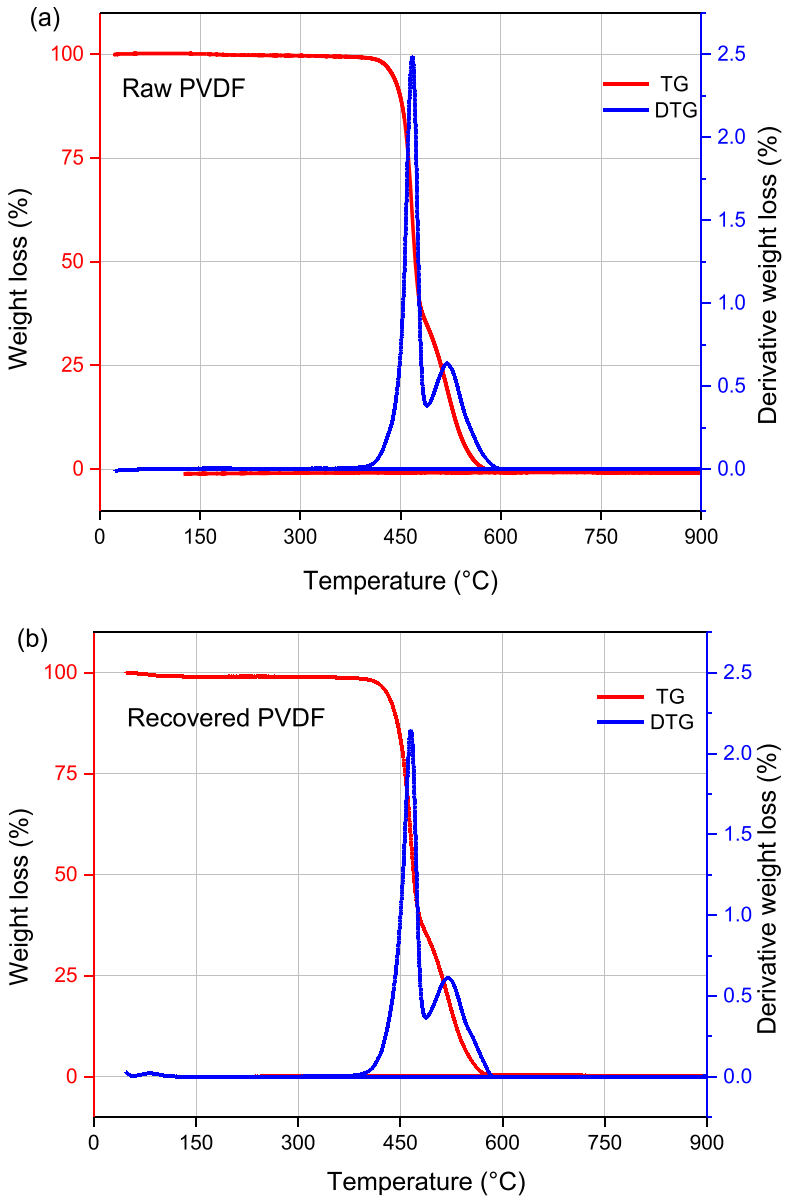

Fig. 5. TG-DTG curve of (a) raw and (b) recovered PVDF

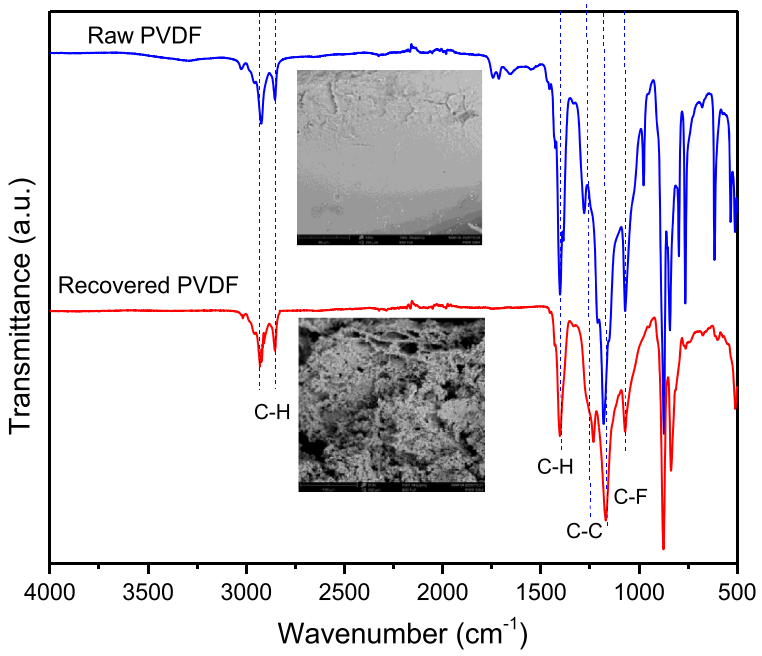

Fig. 6. FTIR spectra with corresponding SEM images of raw and recovered PVDF

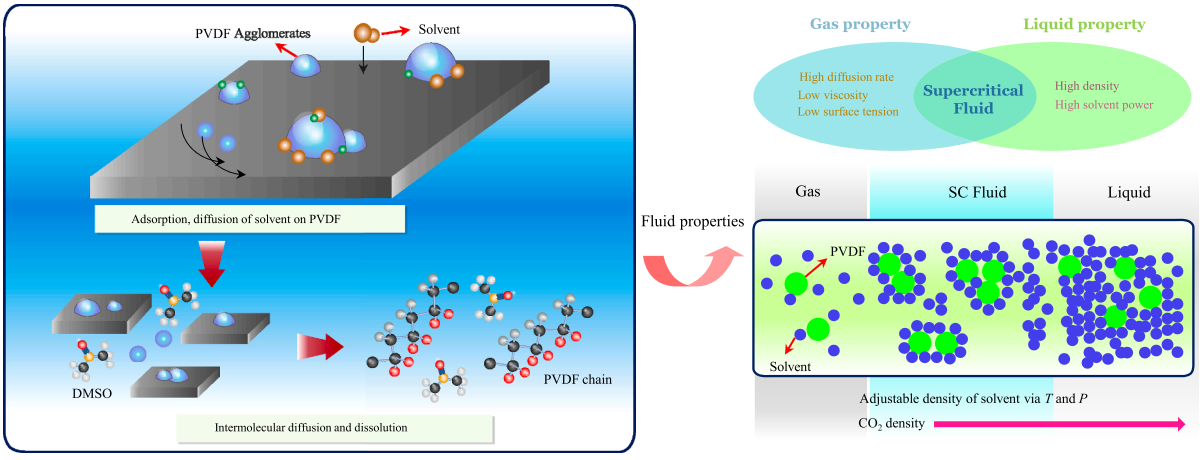

Fig. 7. Schematic representation of PVDF dissolution in supercritical CO_2 process

high solubility of non-polar compounds, and a high mass transport coefficient (Brunner, 2013) is beneficial for the dissolution of PVDF binder using additional cosolvent.

3.3. De-agglomeration and liberation of cathode material via SC CO_2 treatment

3.3.1. Morphology of cathode material before and after SC CO_2 treatment

De-agglomeration and dispersibility characteristics of cathode material were studied by the removal of PVDF binder using SC CO_2 at 80 bar and 70°C for 13 min. Samples were analyzed by SEM before and after Sc-CO_2 treatment, and the micrographs are given in Fig. 8. As it is expected, cathode particles are adhered by the binder and form the spherical secondary particles and particle clusters (Fig. 8a). The higher magnification SEM image (Fig. 8b) for the pristine sample displays that particle size distribution varies between 5 and 20 μm. The EDS analyses detected carbon, oxygen, and metal (cobalt, nickel, and manganese) containing phase in the aggregated particles around point 1 in Fig. 8b, the existence of cathode material. In comparison, fluorine and carbon are highly enriched around point 2. It is known that fluorine and carbon are the main content of PVDF, and the existence of the organic PVDF film can be identified by the distribution of these elements (Yu et al., 2018, Zhang et al., 2014). Considering the EDS spectrum, blurry parts of the Fig. 8a and b are clear evidence of PVDF covering the surface of cathode powders. After SC CO_2 treatment, in Fig. 8c and d, it can be observed that large particle clusters became smaller. The agglomeration

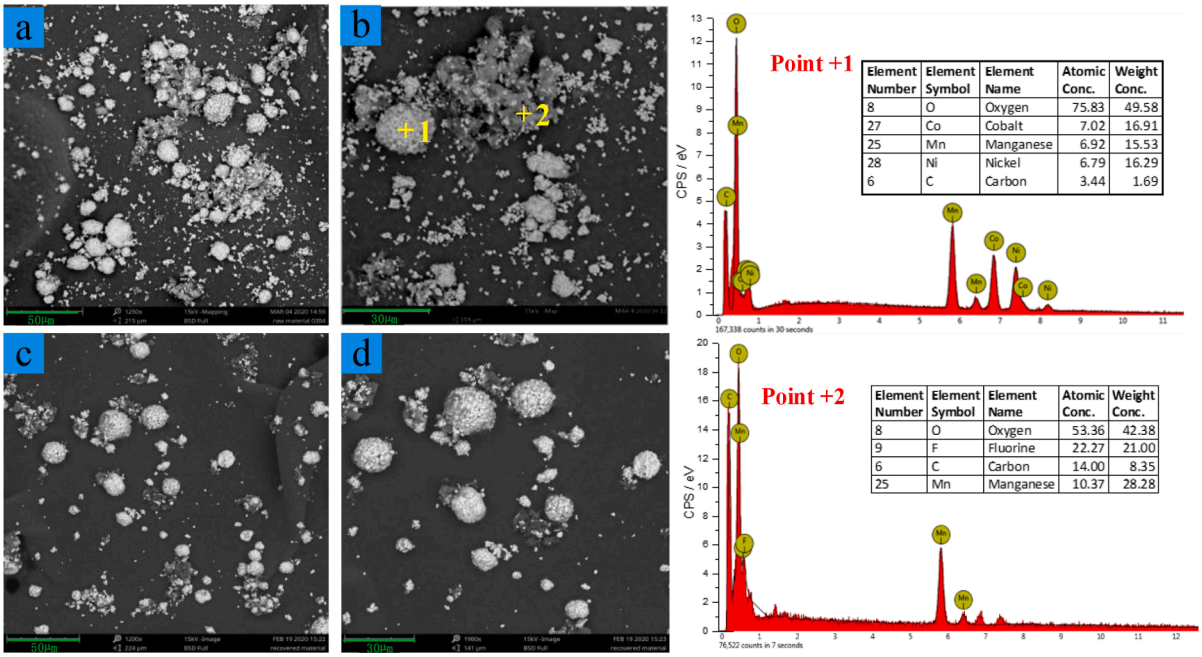

Fig. 8. SEM-EDS images of cathode material before (a, b) and after (c, d) SC CO_2 treatment

decreased by removing of organic binder, and thus the cathode particles are dispersed into a smaller fragment.

3.3.2. Liberation effect of cathode material before and after SC CO_2 treatment

The effect of SC CO_2 extraction using DMSO cosolvent on the size distribution of the cathode materials were also evaluated by the sieving process, and the results are shown in Fig. 9a. The fine fraction with -75 μm size accounts for 21.63 wt% in the raw cathode material. The higher content of coarse size fraction indicates that some cathode materials cannot liberate from foils due to agglomeration between particles and binders. After SC CO_2 treatment, the coarse size fraction (+75 μm) decreased to 67.55% compared to the raw cathode material, which is 78.37%. Besides, the finer size fraction (-45 μm) in the raw cathode is only 6.1%, while it increased to 14.48% after SC CO_2 treatment. Fig. 9b presents the DTG curves of cathode material before and after SC CO_2 treatment. It is obvious that the peaks of electrolyte and PVDF disappeared after treatment, which indicates organic binders and electrolyte were removed successfully. The size distribution and TGA denote that removal of PVDF by SC CO_2 with the cosolvent method is useful for cathode material liberation. Based on the above morphology and size distribution analysis, SC CO_2-DMSO fluid system is confirmed effective for de-agglomeration and liberation of cathode material. Compared with the previous studies stated in the introduction, lower temperature and time are sufficient for effective PVDF removal by the SC CO_2 process, which has relatively low energy consumption and environmentally friendly method to recover organic binder from spent LIBs.

4. Conclusion

In this study, supercritical CO_2 combined with a cosolvent dimethyl sulfoxide (DMSO) was adapted to extract PVDF binders from spent LIBs cathodes and facilitate the liberation of the cathode material from aluminum foil. The experimental results indicate that 98.5 wt% pure PVDF was dissolved using a supercritical CO_2- DMSO system under the optimum conditions of 70°C temperature, 80 bar pressure, and 13 min process time. The dissolution effect under SC CO_2 treatment is found more effective than under room pressure. The FTIR and TG characterization results revealed that the recovered polyvinylidene fluoride remained the same surficial chemical groups and content as the raw PVDF, which is beneficial for the complete recycling and re-utilization of organics recycled from spent LIBs. The proposed mechanism of supercritical CO_2 on PVDF recovery was raised based on the experimental and characterization results. Further, the liberation effect between cathode material and aluminum foil was conducted under the optimal conditions of SC CO_2 fluid treatment. SEM characterization revealed that the degree of agglomeration decreased significantly owing to the removal of organic binder and the cathode particles are dispersed into smaller size fragments. Meanwhile, the size distribution analysis of the SC CO_2 product also demonstrates that it is of advantage for the cathode material liberation. The suggested process is an effective and sustainable approach to recycle organic binder and liberate cathode material from spent LIBs.

CRediT authorship contribution statement

Yuanpeng Fu: Data curtion, Formal analysis, Writing – original draft, Conceptualization, Methodology, Writing – review & editing. **Jonas Schuster:** . **Martina Petranikova:** Conceptualization, Writing – review & editing. **Burçak Ebin:** Conceptualization, Methodology, Writing – review & editing, Supervision.

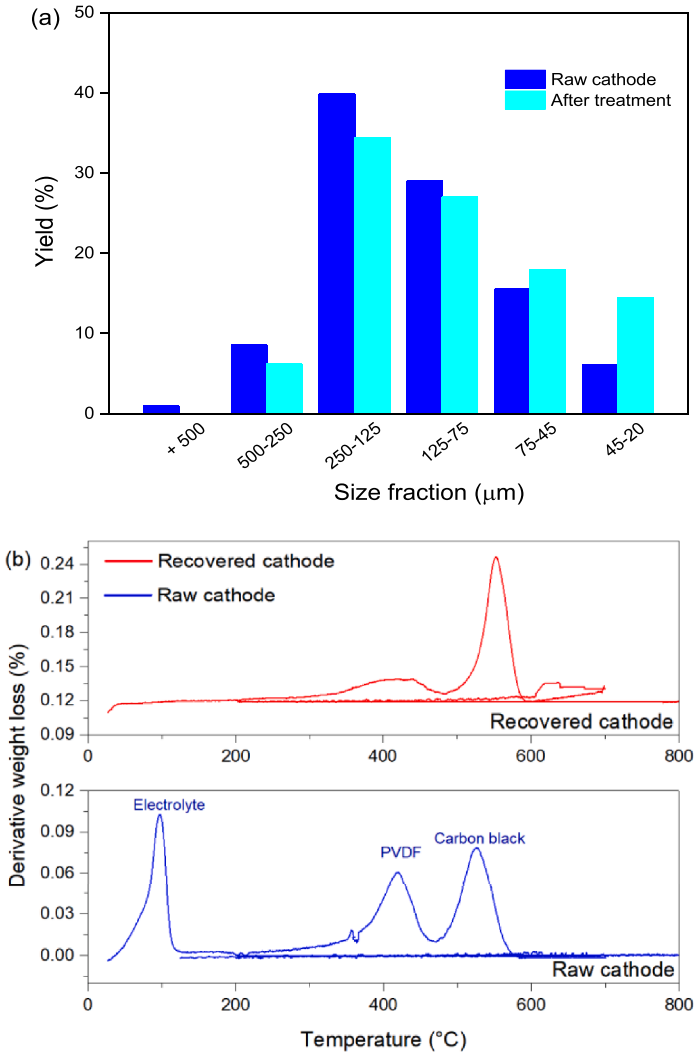

Fig. 9. (a) Size distribution and (b) DTG curves of cathode material before and after SC CO_2 treatment

Declaration of competing interest

The authors declare that they have no known competing financial interests or personal relationships that could have appeared to influence the work reported in this paper.

Acknowledgements

This study is supported by the Swedish Energy Agency Battery Fund Program (Project No: 50124-1). The authors would like to thank the China Scholarship Council (CSC) for supporting Yuanpeng Fu as an exchange PhD student at the Chalmers University of Technology.

Supplementary materials

Supplementary material associated with this article can be found, in the online version, at doi:10.1016/j.resconrec.2021.105666.

References

Shin, S.M., Kim, N.H., Sohn, J.S., Yang, D.H., Kim, Y.H., 2005. Development of a metal recovery process from Li-ion battery wastes. Hydrometallurgy 79 (3-4), 172–181.
Ramanayaka, S., Keerthanan, S., Vithanage, M., 2020. Urban mining of E-waste: treasure hunting for precious nanometals. Handbook of Electronic Waste Management. Butterworth-Heinemann, pp. 19–54.
... Fu, Y., He, Y., Qu, L., Feng, Y., Li, J., Liu, J., Xie, W., 2019. Enhancement in leaching process of lithium and cobalt from spent lithium-ion batteries using benzenesulfonic acid system Waste Manag. 88, 191–199.
Kasnatscheew, J., Wagner, R., Winter, M., Cekic-Laskovic, I., 2018. Interfaces and materials in lithium ion batteries: challenges for theoretical electrochemistry. Model. Electrochem. Energy Storage Atomic Scale 23–51.
Projected lithium ion battery market size worldwide in 2017 and 2025. 2019 https://www-statista-com.proxy.lib.chalmers.se/statistics/235316/global-lithium-battery-market/ (accessed 19. 08. 09).
Zhang, X., Cao, H., Xie, Y., Ning, P., An, H., You, H., Nawaz, F., 2015. A closed-loop process for recycling $LiNi_{1/3}Co_{1/3}Mn_{1/3}O_2$ from the cathode scraps of lithium-ion batteries: Process optimization and kinetics analysis. Separat. Purificat. Technol. 150, 186–195.
Meng, Q., Zhang, Y., Dong, P., Liang, F., 2018. A novel process for leaching of metals from $LiNi_{1/3}Co_{1/3}Mn_{1/3}O_2$ material of spent lithium ion batteries: Process optimization and kinetics aspects. J. Ind. Eng. Chem. 61, 133–141.
Shi, Y., Chen, G., Chen, Z., 2018. Effective regeneration of $LiCoO_2$ from spent lithium-ion batteries: a direct approach towards high-performance active particles. Green chemistry 20 (4), 851–862.
Meshram, P., Pandey, B.D., Mankhand, T.R., 2015. Hydrometallurgical processing of spent lithium ion batteries (LIBs) in the presence of a reducing agent with emphasis on kinetics of leaching. Chem. Eng. J. 281, 418–427.
Meshram, P., Pandey, B.D., Mankhand, T.R., 2015. Recovery of valuable metals from cathodic active material of spent lithium ion batteries: Leaching and kinetic aspects. Waste Manag. 45, 306–313.
... Fu, Y., He, Y., Chen, H., Ye, C., Lu, Q., Li, R., Wang, J., 2019. Effective leaching and extraction of valuable metals from electrode material of spent lithium-ion batteries using mixed organic acids leachant J. Ind. Eng. Chem. 79, 154–162.
Yang, L., Xi, G., Xi, Y., 2015. Recovery of Co, Mn, Ni, and Li from spent lithium ion batteries for the preparation of LiNixCoyMnzO2 cathode materials. Ceramics Int. 41 (9), 11498–11503.

Zhang, G., He, Y., Feng, Y., Wang, H., Zhang, T., Xie, W., Zhu, X., 2018. Enhancement in liberation of electrode materials derived from spent lithium-ion battery by pyrolysis. J. Clean. Prod. 199, 62–68.
... Ku, H., Jung, Y., Jo, M., Park, S., Kim, S., Yang, D., Kwon, K., 2016. Recycling of spent lithium-ion battery cathode materials by ammoniacal leaching J. Hazard. Mater. 313, 138–146.
Zhang, T., He, Y., Ge, L., Fu, R., Zhang, X., Huang, Y., 2013. Characteristics of wet and dry crushing methods in the recycling process of spent lithium-ion batteries. J. Power Sour. 240, 766–771.
Li, J., Shi, P., Wang, Z., Chen, Y., Chang, C.C., 2009. A combined recovery process of metals in spent lithium-ion batteries. Chemosphere 77 (8), 1132–1136.
Xin, Y., Guo, X., Chen, S., Wang, J., Wu, F., Xin, B., 2016. Bioleaching of valuable metals Li, Co, Ni and Mn from spent electric vehicle Li-ion batteries for the purpose of recovery. J. Clean. Prod. 116, 249–258.
Nayaka, G.P., Pai, K.V., Manjanna, J., Keny, S.J., 2016. Use of mild organic acid reagents to recover the Co and Li from spent Li-ion batteries. Waste Manag. 51, 234–238.
Hao, J., Wang, H., Chen, S., Cai, B., Ge, L., Xia, W., 2014. Pyrolysis characteristics of the mixture of printed circuit board scraps and coal powder. Waste Manag. 34 (10), 1763–1769.
Choi, S.S., Kim, Y.K., 2012. Microstructural analysis of poly (vinylidene fluoride) using benzene derivative pyrolysis products. J. Anal. Appl. Pyrolys. 96, 16–23.
Lombardo, G., Ebin, B., Foreman, M.R.S.J., Steenari, B.M., Petranikova, M, 2020. Incineration of EV Lithium-ion batteries as a pretreatment for recycling–determination of the potential formation of hazardous by-products and effects on metal compounds. J. Hazard. Mater., 122372
Zhang, G., He, Y., Feng, Y., Wang, H., Zhu, X., 2018. Pyrolysis-ultrasonic-assisted flotation technology for recovering graphite and LiCoO2 from spent lithium-ion batteries. ACS Sustain. Chem. Eng. 6 (8), 10896–10904.
Hanisch, C., Loellhoeffel, T., Diekmann, J., Markley, K.J., Haselrieder, W., Kwade, A., 2015. Recycling of lithium-ion batteries: a novel method to separate coating and foil of electrodes. J. Clean. Prod. 108, 301–311.
Risk Evaluation for N-Methylpyrrolidone (NMP) https://www.epa.gov/assessing-and-managing-chemicals-under-tsca/risk-evaluation-n-methylpyrrolidone-nmp-0 (accessed 19. 12. 2016)).
Lv, W., Wang, Z., Cao, H., Sun, Y., Zhang, Y., Sun, Z., 2018. A critical review and analysis on the recycling of spent lithium-ion batteries. ACS Sustain. Chem. Eng. 6 (2), 1504–1521.
Grützke, M., Mönnighoff, X., Horsthemke, F., Kraft, V., Winter, M., Nowak, S., 2015. Extraction of lithium-ion battery electrolytes with liquid and supercritical carbon dioxide and additional solvents. RSC Adv. 5 (54), 43209–43217.
Sanyal, S., Ke, Q., Zhang, Y., Ngo, T., Carrell, J., Zhang, H., Dai, L.L., 2013. Understanding and optimizing delamination/recycling of printed circuit boards using a supercritical carbon dioxide process. J. Clean. Prod. 41, 174–178.
Xiu, F.R., Zhang, F.S., 2009. Recovery of copper and lead from waste printed circuit boards by supercritical water oxidation combined with electrokinetic process. J. Hazard. Mater. 165 (1-3), 1002–1007.
Xing, M., Zhang, F.S., 2013. Degradation of brominated epoxy resin and metal recovery from waste printed circuit boards through batch sub/supercritical water treatments. Chem. Eng. J. 219, 131–136.
Wang, M., Tan, Q., Chiang, J.F., Li, J., 2017. Recovery of rare and precious metals from urban mines—a review. Front. Environ. Sci. Eng. 11 (5), 1.
Cooper, A.I., 2000. Polymer synthesis and processing using supercritical carbon dioxide. J. Mater. Chem. 10, 207–234.
Lin, F., Liu, D., Maiti Das, S., Prempeh, N., Hua, Y., Lu, J., 2014. Recent progress in heavy metal extraction by supercritical CO_2 fluids. Ind. Eng. Chem. Res. 53 (5), 1866–1877.
Xiang, Y., Xue, L., Shen, J., Lin, H., Liu, F., 2014. Effect of solvents on morphology and polymorphism of polyvinylidene fluoride membrane via supercritical CO_2 induced phase separation. J. Appl. Polym. Sci. 131 (22).
Herrero, M., Mendiola, J.A., Cifuentes, A., Ibáñez, E., 2010. Supercritical fluid extraction: recent advances and applications. J. Chromatogr. A 1217 (16), 2495–2511.
Erkey, C., 2000. Supercritical carbon dioxide extraction of metals from aqueous solutions: a review. J. Supercritic. Fluids 17 (3), 259–287.
... Baek, D.L., Fox, R.V., Case, M.E., Sinclair, L.K., Schmidt, A.B., McIlwain, P.R., Wai, C. M., 2016. Extraction of rare earth oxides using supercritical carbon dioxide modified with Tri-n-butyl phosphate–nitric acid adducts Ind. Eng. Chem. Res. 55 (26), 7154–7163.
Lin, F., Liu, D., Maiti Das, S., Prempeh, N., Hua, Y., Lu, J., 2014. Recent progress in heavy metal extraction by supercritical CO_2 fluids. Ind. Eng. Chem. Res. 53 (5), 1866–1877.
Liu, Y., Mu, D., Li, R., Ma, Q., Zheng, R., Dai, C., 2017. Purification and characterization of reclaimed electrolytes from spent lithium-ion batteries. J. Phys. Chem. C 121 (8), 4181–4187.
Nowak, S., Winter, M., 2017. The role of sub-and supercritical CO_2 as "Processing Solvent" for the recycling and sample preparation of lithium ion battery electrolytes. Molecules 22 (3), 403.
Argenta, A.B., Reis, C.M., Mello, G.P., Dotto, G.L., Tanabe, E.H., Bertuol, D.A., 2017. Supercritical CO_2 extraction of indium present in liquid crystal displays from discarded cell phones using organic acids. J. Supercritic. Fluids 120, 95–101.
... Grützke, M., Kraft, V., Weber, W., Wendt, C., Friesen, A., Klamor, S., Nowak, S., 2014. Supercritical carbon dioxide extraction of lithium-ion battery electrolytes J. Supercritic. Fluids 94, 216–222.
Bertuol, D.A., Machado, C.M., Silva, M.L., Calgaro, C.O., Dotto, G.L., Tanabe, E.H., 2016. Recovery of cobalt from spent lithium-ion batteries using supercritical carbon dioxide extraction. Waste Manag. 51, 245–251.
Marr, R., Gamse, T., 2000. Use of supercritical fluids for different processes including new developments—a review. Chem. Eng. Process. 39 (1), 19–28.
Nieuwoudt, M.K., Simpson, M.P., Tobin, M., Puskar, L., 2014. Synchrotron FTIR microscopy of synthetic and natural CO2–H2O fluid inclusions. Vibrat. Spectrosc. 75, 136–148.
He, L.P., Sun, S.Y., Song, X.F., Yu, J.G., 2015. Recovery of cathode materials and Al from spent lithium-ion batteries by ultrasonic cleaning. Waste Manag. 46, 523–528.
Zhan, R., Payne, T., Leftwich, T., Perrine, K., Pan, L., 2020. De-agglomeration of cathode composites for direct recycling of Li-ion batteries. Waste Manag. 105, 39–48.
Talebi, S., 2008. Disentangled Polyethylene with Sharp Molar Mass Distribution: Implications for Sintering. Technische Universiteit Eindhoven. https://doi.org/10.6100/IR639413.
Bachu, S., 2008. CO_2 storage in geological media: Role, means, status and barriers to deployment. Progr. Energy Combust. Sci. 34 (2), 254–273.
Brunner, G., 2013. Gas Extraction: an Introduction to Fundamentals of Supercritical Fluids and the Application to Separation Processes (Vol. 4). Springer Science & Business Media.
Yu, J., He, Y., Ge, Z., Li, H., Xie, W., Wang, S., 2018. A promising physical method for recovery of LiCoO2 and graphite from spent lithium-ion batteries: grinding flotation. Separat. Purificat. Technol. 190, 45–52.
Zhang, T., He, Y., Wang, F., Li, H., Duan, C., Wu, C., 2014. Surface analysis of cobalt-enriched crushed products of spent lithium-ion batteries by X-ray photoelectron spectroscopy. Separat. Purificat. Technol. 138, 21–27.